Journal of Materials Chemistry A

Accepted Manuscript

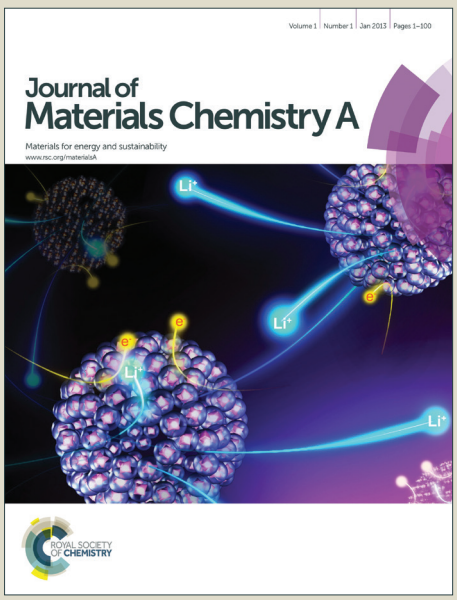

ROYAL SOCIETY OF CHEMISTRY

www.rsc.org/materialsA

Journal Name

RSCPublishing

COMMUNICATION

Three Dimensional Palladium Nanoflowers with Enhanced Electrocatalytic Activity towards the Anodic Oxidation of Formic Acid

Cite this: DOI: 10.1039/x0xx00000x

Received 00th January 2012,
Accepted 00th January 2012

DOI: 10.1039/x0xx00000x

www.rsc.org/

Bingqing Zhang,[a,b] Hongliang Peng,[a] Lijun Yang,[a] Hualing Li,[a] Haoxiong Nan,[a] Zhenxing Liang,[a] Huiyu Song,[a] Huaneng Su,[a] Can Li,*[b] and Shijun Liao*[a]

A three-dimensional palladium nanoflowers (Pd-NF) composed of ultrathin Pd nanosheets was synthesized by a solvothermal approach. The Pd-NF catalyst shows 6.6- and 5.5- folds mass activity and surface activity of normal palladium nanoparticle (Pd-NP) in electric oxidation of formic acid.

The electro-oxidation of formic acid has attracted much attention in last decades due to the advantages and potentially wide applications of direct formic acid fuel cell (DFAFC).[1-6] Many works on the electro-oxidation of formic acid have been done on platinum- and palladium-based catalysts because they are recognized as the best anode catalysts. But Pt catalyst, is considered not to be an appropriate catalyst for DFAFC due to they are easily poisoned by intermediate CO species formed in formic acid oxidizing process. Nevertheless, Pd is more attractive than Pt due to the lower cost and less poisoning,[4] especially at lower anode potentials (<0.4 V vs. RHE) in the electro-oxidation of formic acid.

The issues including size, shape, architecture, crystallographic features and specific crystal planes are considered to be the key factors determining material properties and functions.[7-10] In recent years, the fabrication and application of unique morphology Pd nanomaterial have attracted much attention. Most of the published work were focused on zero-dimensional (such as nanoparticle[11-15]), one-dimensional (such as nanowire,[16-20] nanorod,[16,21] or nanotubular[22]) and two-dimensional (nanosheet[23-26]) Pd nanostructure. Among the diverse nano-architectures, three-dimensional Pd nanostructure has emerged as promising materials due to possess a porous nature, a large surface areas and active centers for electrocatalysis.[7,27-37] Arjona[38] used electrochemical method synthesized flower-like Pd nanoparticles showed high tolerance toward formic acid electrooxidation. Yu et al[37] used a very simple chemical method to fabricate branched Pd nanodendrites, which had displayed substantially enhanced the activity of both oxygen reduction reaction and methanol oxidation compared with that of commercial Pd/C catalysts. Most of the reported three-dimensional Pd nanostructures are the assembly of nanoparticle or nanowire or nanorod, as far as we know, there is no report on the three-dimensional Pd nanostructure which assemble by two-dimensional Pd nanosheets.

In this work, we synthesized a three-dimensional Pd nanoflower (denoted as Pd-NF) which is the assembly of ultrathin nanosheets by a mild and simple solvothermal approach. A precursor solution was prepared by dissolving palladium chloride into benzyl alcohol solvent, and added oleic acid as the template. The mixture was then placed into a Teflon®-lined autoclave, followed by a solvothermal reaction at 140ºC for 6 hours. For comparison, Pd nanoparticle (Pd-NP) was prepared by the same procedure without adding oleic acid.

Figure 1a presents the scanning electron microscope (SEM) image of Pd nanoparticle without adding oleic acid in the synthesis process. The diameter of Pd-NPs are 200 nm ± 50 nm, the aggregation of these nanoparticles occurs. However, after adding oleic acid, the sample displays a perfect nanoflower morphology (Figure 1b,c). The nanoflowers show the uniform size distribution of 500 ± 100 nm. The high resolution scanning

electron microscope (HR-SEM) image of Figure 1d shows that the nanoflowers are the assembly of ultrathin Pd nanosheets. The average thickness of Pd nanosheets in Figure 1d is *ca.* 4−8 nm, and the size of Pd nanosheets is roughly estimated to be about hundreds of nanometers. The high resolution transmission electron microscope (HR-TEM) images in Figure 1e and 1f well confirmed that the Pd nanoflowers are the assembly of thin Pd nanosheets. Figure 1e shows a few layers

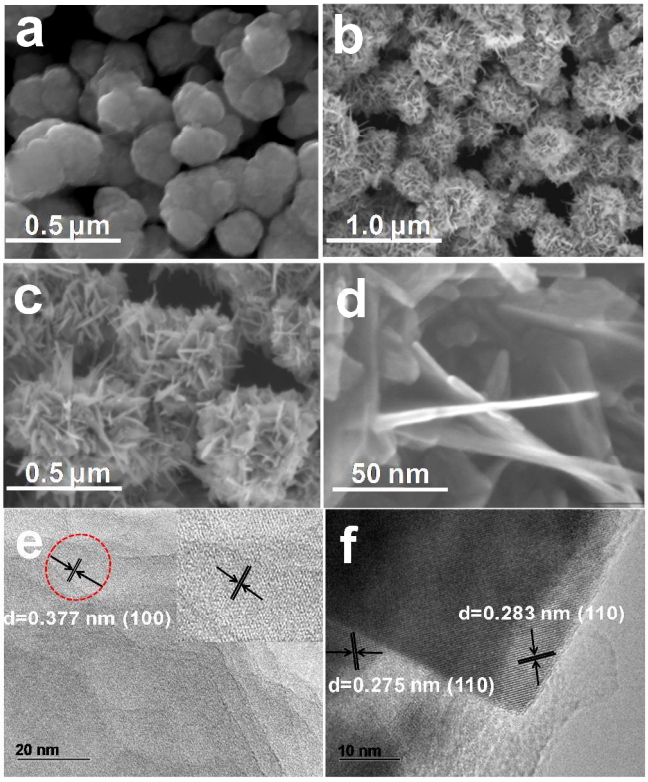

Figure 1. SEM images of Pd-NP (a) and Pd-NF (b, c); HR-SEM image of Pd-NF (d); HR-TEM images of Pd-NF (e, f). The insert image in (e) is the magnification image of the red circle region in (e).

of nanosheets with different lateral sizes randomly overlapping each other, the nanosheets possess lattice spacing of 0.377 and 0.283 nm, which could be assigned to the (100) and (110) planes of Pd.

Compared with Pd-NP, although the size of Pd-NF is larger, but is not the aggregation between flowers. Interestingly, when the reaction time is controlled at 90min (Figure S1b), except for the rough surface, the morphology and the size of Pd-NF is almost the same as Pd-NP (Figure 1a). The result indicating that Pd-NF and Pd-NP are formed maybe through the same nucleation stage.

To better understand the growth mechanism of Pd nanoflower, the time-dependent morphological evolution was followed by SEM measurements (see Figure S1).Almost no products could be obtained when the reaction duration is less than 60 min. When the reaction duration increased to 70 min, the yield of Pd products could be *ca.* 20%, the Pd nanoparticles with particle size of *ca.* 50 nm but not Pd nanoflowers were obtained. Even the duration is increased to 90 min (Figure S1b), only nanoparticles but nit nanoflower can be observed, but the nanoparticles obviously grow up and formed the aggregation of Pd nanoparticles with an average size of 200−250 nm, meanwhile, the surface of nanoparticle is very rough, in the red circle region, a small number of short nanosheets are formed on the surface. However, once the reaction duration is up to 2 h (Figure S1c), we can see the anisotropic grow that nanoparticles surface resulting in the formation of nanosheets, with the size up to 400−500 nm. When the duration is up to 3h, the nanosheets grow further and more flower-like nanostructures can be observed (Figure S1d). We found that the beautiful nanoflower with uniform size distribution of 500 ± 100 nm can be observed when the reaction duration gets up to 6h. Clearly, the formation of the nanoflowers is a template directed and slow process.

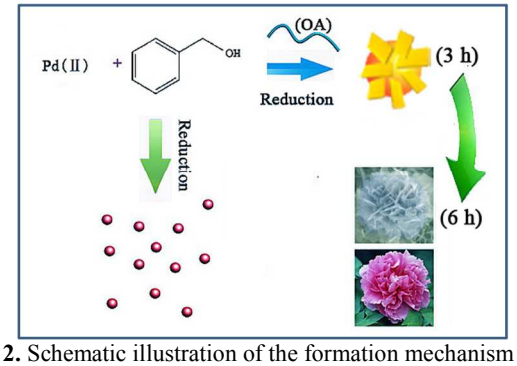

Figure 2. Schematic illustration of the formation mechanism of a Pd nanoflower.

According to the SEM and TEM images shown in Figure 1 and Figure S1, a possible formation process of the Pd nanoflowers is proposed (Figure 2). First, Pd nanonuclei are formed in solution through the reduction of $PdCl_2$ by benzyl alcohol, the nuclei tend to grow and aggregate into normal particles without the template. When the oleic acid is added as a capping agent, on one hand, the Pd nuclei grow up to nanoparticles; On the other hand, direction agent restraint the growth and began develop into nanosheets, with the prolonged reaction time, the material finally grow into nanoflowers structure, which are assembly of ultrathin nanosheets.

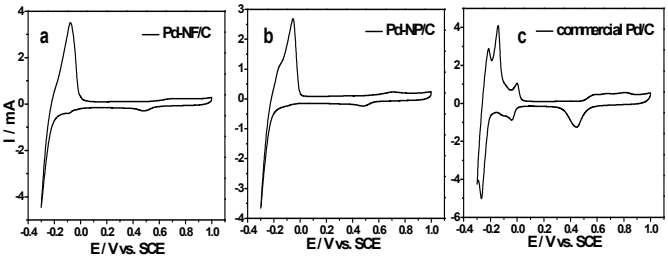

Figure 3. The cyclic voltammetry curve for Pd-NF/C (a), Pd-NP/C (b) and commercial Pd/C (c) in N_2-saturated 0.5 M H_2SO_4 solution with a scan rate of 50 mV s^{-1}. The mass ratio of Pd in Pd/C are 20 *wt.*% for all samples and the loading of Pd on electrode is 0.1 mg.

To investigate the electrocatalytic properties of the obtained samples, we supported them on carbon material (XC-72) and the metal loading are 20 *wt.*%. Figure 3 show the Cyclic voltammetry (CV) of Pd-NF/C, Pd-NP/C and commercial Pd/C (BASF, 20 *wt.*%) catalysts in background solution (0.5 M H_2SO_4). The peaks in -0.3−0V (*vs.* SCE) are attributed to the hydrogen adsorption, desorption and evolution, respectively, they are not well-separated of Pd-NF/C and Pd-NP/C catalysts, so the hydrogen adsorption–desorption processes are not appropriate for evaluate electrochemical active surface area (ECSA) of Pd. The oxygen adsorption method is usually applicable to evaluate ECSA of metals that showing well-developed regions for oxide monolayer formation and reduction, such as Au and Pd.[3,39,40] In Figure 3, the cathodic curve of Pd-NF/C, Pd-NP/C and commercial Pd/C present a Pd surface oxide reduction peak at 0.49, 0.49, and 0.45 V, the reduction charge is integrated to be 1047.4, 869.1 and 3844.3 μC, after divided by conversion factor of 424 μC cm^{-2} (the charge that needed to form surface oxide monolayer),[39,41] the corresponding active surface area is 2.47, 2.05, and 9.07 cm^2, respectively. The result shows that the Pd-NF and Pd-NP with the almost same surface area, much lower than that of the commercial Pd/C.

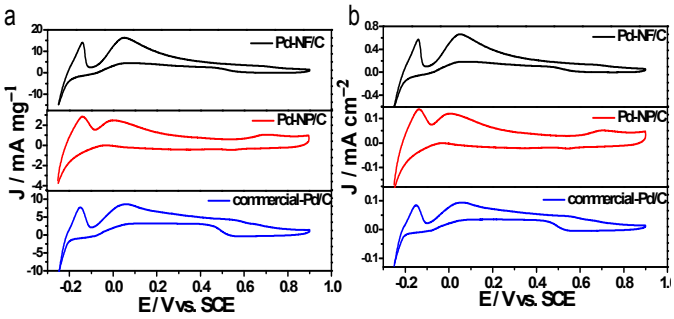

Figure 4. The electro-oxidation of formic acid activity normalized by the mass (a) and ECSA (b) of Pd for Pd-NF/C, Pd-NP/C and commercial Pd/C (BASF) in N_2-saturated 0.5 M H_2SO_4 + 0.5 M HCOOH solution with a scan rate of 20 mV s^{-1}. The loading of Pd on electrode is 0.1 mg for all samples and the ECSA of Pd-NF/C, Pd-NP/C and commercial Pd/C are 2.47, 2.05, and 9.07 cm^2, respectively.

Table 1. The comparison of Pd-NF/C, Pd-NP/C and Commcial Pd/C for electro-oxidation of formic acid activity

Catalysts	Loading of Pd (mg)	ECSA (cm^2)	Peak current (mA)[a]	Mass activity (mA/mg)	Surface activity (mA /cm^2)
Pd-NF/C	0.1	2.47	1.64	16.4	0.66
Pd-NP/C	0.1	2.05	0.25	2.5	0.12
BASF-Pd/C	0.1	9.07	0.85	8.5	0.09

[a] The formic electro-oxidation peak current of the 10th cycle in Figure S2.

Figure 4 shows the formic acid oxidation activities of Pd-NF/C and Pd-NP/C catalysts, as well as commercial Pd/C catalyst. Due to Pd easily dissolve in an acid electrolyte during the oxidation-reduction,[42] to be fair, several cycles are recorded in cyclic voltammetry measurement for each sample (Figure S2), we adopt the relative stable cycle (the 10th cycle) for discussion. Obviously, all of them have two sharp anodic direction peaks and a broad cathodic direction peak. In general, the anodic direction peaks at −0.14 V and 0.05 V correspond to the hydrogen desorption and the activity of direct oxidation of formic acid, the broad cathodic direction peak reflect the stripping of the absorbed intermediates and regeneration of the Pd surface.[41,43,44] Except for the peak of direct oxidation of formic acid, it is worth mentioning that there is a minor hump at 0.5−0.7 V (*vs.* SCE), which is due to the oxidation of Pd. On the negative scan, firstly reduction of Pd oxide, then followed the oxidation of formic acid on newly reduced Pd surfaces at more broad negative potentials.[45]

The activity of electro-oxidation formic acid can be normalized by the mass and electrochemical active surface area of Pd. The normalized activities are summarized in Table 1. Figure 4a shows the mass activity of Pd-NF/C is as high as 16.4 mA mg^{-1}, 6.6 times that of Pd-NP/C and 1.9 times of commercial Pd/C catalyst. When the anodic peak current normalized by ECSA of catalyst (Figure 4b), surprisingly, the intrinsic activity of Pd-NF/C is 7.3 times of commercial Pd/C, which indicate that the much higher activity for Pd-NF than commercial Pd/C on each active site. In addition, we observed the morphology of Pd-NF after hundred CV cycles for the electro-oxidation of formic acid, we found that the morphology of the sample did not damage at all after the CV measurements (Figure S3), indicating the excellent stability of the Pd nanoflowers.

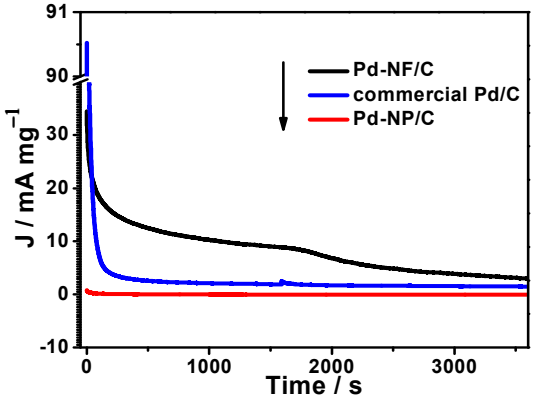

Figure 5. Chronoamperometric curves for the oxidation of formic acid catalyzed by Pd-NF/C, Pd-NP/C and commercial Pd/C at 0.06V (vs. SCE) in N_2-saturated 0.5 M H_2SO_4 + 0.5 M HCOOH solution. The loading of Pd on electrode is 0.1 mg for all samples.

Figure 5 shows the chronoamperometric measurement of Pd-NF/C, Pd-NP/C and commercial Pd/C. The initial current of commercial Pd/C is as high as 90 mA mg^{-1}, 2.6 times that of Pd-NF/C, but it decays very rapidly, is only 4.6 mA mg^{-1} after 160s. The result is in agreement with cyclic voltammetry of electro-oxidation of formic acid activity, in which the peak current is steeply decreased with the increase in the number of

scanning (Figure S2b). On the contrary, the current of Pd-NF/C decayed slowly, although the initial current is lower than those commercial Pd/C, after 60s, the current remains much higher level than those of commercial Pd/C and Pd-NP/C. For Pd-NP/C, the initial current is 0.8 mA mg^{-1}, 40 times lower than Pd-NF/C. Chronoamperometric characterization further verified that Pd-NF/C with the superior mass current density and stability than Pd-NP/C and commercial Pd/C for formic acid oxidation.

In conclusion, a novel Pd nanoflower catalyst, an assembly of ultrathin nanosheet was synthesized by a solvothermal method using oleic acid as template. In electro-oxidation formic acid for direct formic acid fuel cell, the Pd-NF catalyst exhibits 6.6- and 1.9- folds mass activity of Pd-NP catalyst and commercial Pd/C, 5.5- and 7.3- folds surface activity of Pd-NP catalyst and commercial Pd/C, respectively. This result reveals that the intrinsic activity of Pd-NF is much higher than Pd-NP mainly because the Pd-NF is composed of nanosheets with specially exposed facets.

Acknowledgements

This work was supported by the National Science Foundation of China (NSFC Project Nos. 20876062, 21076089, 21276098, 11132004) and Ministry of Science and Technology of China (Project No 2012AA053402).

Notes and references

[a] *The Key Laboratory of Fuel Cell Technology of Guangdong Province & The Key Laboratory of New Energy Technology of Guangdong Universities, School of Chemistry and Chemical Engineering, South China University of Technology, Guangzhou, Guangdong, P. R. China; E-mail: chsjliao@scut.edu.cn*

[b] *State Key Laboratory of Catalysis, Dalian Institute of Chemical Physics, Chinese Academy of Sciences, Dalian National Laboratory for Clean Energy, Dalian, Liaoning, P. R. China; Fax: +86-411-84694447; E-mail: canli@dicp.ac.cn*

† Electronic Supplementary Information (ESI) available: Experimental details, chracterazation. See DOI: 10.1039/b000000x/

1 H. Meng, F. Xie, J. Chen and P. K. Shen, *J. Mater. Chem.*, 2011, **21**, 11352−11358.
2 P. Hong, S. Liao, J. Zeng and X. Huang, *J. Power Sources*, 2010, **195**, 7332−7337.
3 J. Chai, F. Li, Y. Bao, S. Liu, Q. Zhang and L. Niu, *J. Solid State Electrochem.*, 2011, **16**, 1203−1210.
4 V. Mazumder and S. Sun, *J. Am. Chem. Soc.*, 2009, **131**, 4588−4589.
5 W. P. Zhou, A. Lewera, R. Larsen, R. I. Masel, P. S. Bagus and A. Wieckowski, *J. Phys. Chem. B*, 2006, **110**, 13393−13398.
6 J. L. Haan, K. M. Stafford and R. I. Masel, *J. Phys. Chem. C*, 2010, **114**, 11665−11672.
7 S. Guo and E. Wang, *Nano Today*, 2011, **6**, 240-264.
8 Y. Xia, Y. Xiong, B. Lim and S. E. Skrabalak, *Angew. Chem. Int. Ed.*, 2009, **48**, 60−103.
9 X. Lu, M. Rycenga, S. E. Skrabalak, B. Wiley and Y. Xia, *Annu. Rev. Phys. Chem.*, 2009, **60**, 167−192.
10 H. Zhang, M. Jin, Y. Xiong, B. Lim and Y. Xia, *Acc. Chem. Res.*, 2012, **46**, 1783−1794.
11 A. R. Siamaki, A. E. R. S. Khder, V. Abdelsayed, M. S. El-Shall and B. F. Gupton, *J. Catal.*, 2011, **279**, 1−11.
12 X. Xu, Y. Li, Y. Gong, P. Zhang, H. Li and Y. Wang, *J. Am. Chem. Soc.*, 2012, **134**, 16987−16990.
13 L. Zhang, T. Lu, J. Bao, Y. Tang and C. Li, *Electrochem. Commun.*, 2006, **8**, 1625−1627.
14 Q. Wan, Y. Liu, Z. Wang, W. Wei, B. Li, J. Zou and N. Yang, *Electrochem. Commun.*, 2013, **29**, 29−32.
15 B. H. Mao, C. H. Liu, X. Gao, R. Chang, Z. Liu and S. D. Wang, *Appl. Surf. Sci.*, 2013, **283**, 1076−1079.
16 X. Q. Huang and N. F. Zheng, *J. Am. Chem. Soc.*, 2009, **131**, 4602−4603.
17 P. F. Siril, A. Lehoux, L. Ramos, P. Beaunier and H. Remita, *New J. Chem.*, 2012, **36**, 2135-2139.
18 J. Wang, Y. Chen, H. Liu, R. Li and X. Sun, *Electrochemistry. Commun.*, 2010, **12**, 219−222.
19 C. Koenigsmann, A. C. Santulli, E. Sutter and S. S. Wong, *ACS Nano*, 2011, **5**, 7471−7487.
20 C. Koenigsmann, A. C. Santulli, K. Gong, M. B. Vukmirovic, W. P. Zhou, E. Sutter, S. S. Wong and R. R. Adzic, *J. Am. Chem. Soc.*, 2011, **133**, 9783−9795.
21 C. Xiao, H. Ding, C. Shen, T. Yang, C. Hui and H. J. Gao, *J. Phys. Chem. C*, 2009, **113**, 13466−13469.
22 H. Bai, M. Han, Y. Du, J. Bao and Z. Dai, *Chem. Commun.*, 2010, **46**, 1739−1741.
23 P. F. Siril, L. Ramos, P. Beaunier, P. Archirel, A. Etcheberry and H. Remita, *Chem. .Mater.*, 2009, **21**, 5170−5175.
24 H. Li, G. Chen, H. Yang, X. Wang, J. Liang, P. Liu, M. Chen and N. Zheng, *Angew. Chem. Int. Ed.*, 2013, **52**, 8368−8372.
25 Z. Y. Chen, D. C. Pan, H. F. Wang, M. L. Mao, Y. C. Han and J. Lin, *Nanotechnology*, 2006, **17**, 506-511.
26 X. Huang, S. Tang, X. Mu, Y. Dai, G. Chen, Z. Zhou, F. Ruan, Z. Yang and N. Zheng, *Nat. Nanotechnol.*, 2011, **6**, 28−32.
27 J. Watt, N. Young, S. Haigh, A. Kirkland and R. D. Tilley, *Advanced Materials*, 2009, **21**, 2288−2293.
28 A. J. Wang, F. F. Li, J. N. Zheng, H. X. Xi, Z. Y. Meng and J. J. Feng, *RSC Adv.*, 2013, **3**, 10355-10362.
29 M. Sawangphruk, A. Krittayavathananon, N. Chinwipas, P. Srimuk, T. Vatanatham, S. Limtrakul and J. S. Foord, *Fuel Cells*, 2013, **0**, 1−8.
30 G. M. Yang, X. Chen, J. Li, Z. Guo, J. H. Liu and X. J. Huang, *Electrochim. Acta*, 2011, **56**, 6771−6778.
31 A. Mohanty, N. Garg and R. Jin, *Angew. Chem. Int. Ed.*, 2010, **49**, 4962−4966.
32 J. Watt, S. Cheong, M. F. Toney, B. Ingham, J. Cookson, P. T. Bishop and R. D. Tilley, *ACS Nano*, 2009, **4**, 396−402.
33 Z. Yin, H. Zheng, D. Ma and X. Bao, *J. Phys. Chem. C*, 2008, **113**, 1001−1005.
34 H.P. Liang, N. S. Lawrence, L. J. Wan, L. Jiang, W. G. Song and T. G. J. Jones, *J. Phys. Chem. C*, 2007, **112**, 338−344.
35 L. M. Wang, S. He, Z. M. Cui and L. Guo, *Inorg. Chem. Commun.*, 2011, **14**, 1574−1578.
36 G. Fu, W. Han, L. Yao, J. Lin, S. Wei, Y. Chen, Y. Tang, Y. Zhou, T. Lu and X. Xia, *J. Mater. Chem.*, 2012, **22**, 17604−17611.
37 Q. Gao, M. R. Gao, J. W. Liu, M. Y. Chen, C. H. Cui, H. H. Li and S. H. Yu, *Nanoscale*, 2013, **5**, 3202−3207.
38 N. Arjona, M. Guerra-Balcázar, F. M. Cuevas-Muñiz, L. Álvarez-Contreras, J. Ledesma-García and L. G. Arriaga, *RSC Adv.*, 2013, **3**, 15727−15733.
39 S. Trasatti and O. Petrii, *Pure Appl. Chem.*, 1991, **63**, 711−734.
40 X. Wang, W. Wang, Z. Qi, C. Zhao, H. Ji and Z. Zhang, *Electrochem. Commun.*, 2009, **11**, 1896−1899.
41 W. Pan, X. Zhang, H. Ma and J. Zhang, *J. Phys. Chem. C*, 2008, **112**, 2456−2461.
42 M. Baldauf and D. Kolb, *J. Phys. Chem.*, 1996, **100**, 11375−11381.
43 Y. Zhou, J. Liu, J. Ye, Z. Zou, J. Ye, J. Gu, T. Yu and A. Yang, *Electrochim. Acta*, 2010, **55**, 5024−5027.
44 J. Zhang, C. Qiu, H. Ma and X. Liu, *J. Phys. Chem. C*, 2008, **112**, 13970−13975.
45 H. Meng, S. Sun, J. P. Masse and J. P. Dodelet, *Chem. Mater.*, 2008, **20**, 6998−7002.

Table of Contents

Three Dimensional Palladium Nanoflowers with Enhanced Electrocatalytic Activity towards the Anodic Oxidation of Formic Acid

Bingqing Zhang[a,b], Hongliang Peng [a], Lijun Yang[a], Hualing Li[a], Haoxiong Nan[a], Zhenxing Liang[a], Huiyu Song[a], Huaneng Su[a], Can Li[b,1], Shijun Liao[a,2]

Pd nanoflowers (Pd-NF) composed of ultrathin Pd nanosheets, show significantly enhance the activity of electro-oxidation of formic acid of ordinary Pd nanoparticles.

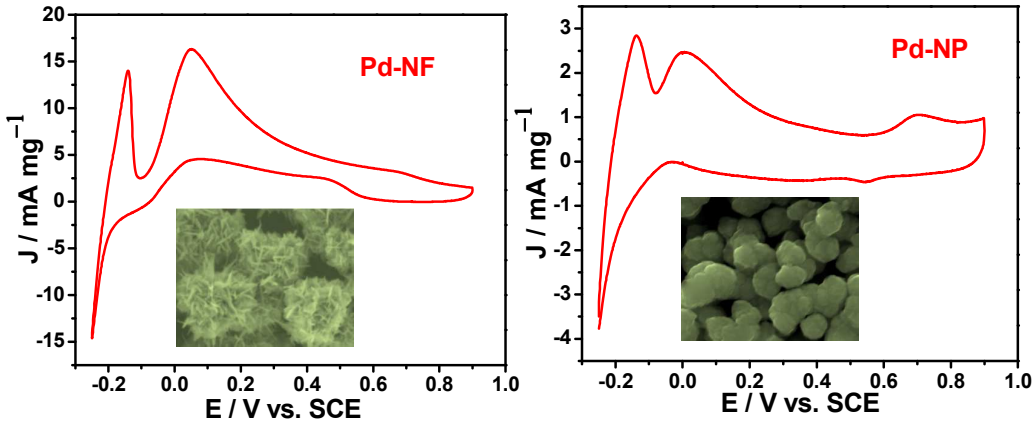

[1] Corresponding author, e-mail: canli@dicp.ac.cn, fax 86 411 84694447
[2] Corresponding author, e-mail: chsjliao@scut.edu.cn, fax 86 20 87113586